



Blue-detuned optical atom trapping in a compact plasmonic structure

ZHAO CHEN,¹ FAN ZHANG,¹ QI ZHANG,¹ JUANJUAN REN,¹ HE HAO,¹ XUEKE DUAN,¹ PENGFEI ZHANG,^{2,3} TIANCAI ZHANG,^{2,3} YING GU,^{1,2,*} AND QIHUANG GONG^{1,2}

¹State Key Laboratory for Mesoscopic Physics, Collaborative Innovation Center of Quantum Matter, Department of Physics, Peking University, Beijing 100871, China

²Collaborative Innovation Center of Extreme Optics, Shanxi University, Taiyuan, Shanxi 030006, China

³State Key Laboratory of Quantum Optics and Quantum Optics Devices, Institute of Opto-Electronics, Shanxi University, Taiyuan 030006, China

*Corresponding author: ygu@pku.edu.cn

Received 17 April 2017; revised 28 June 2017; accepted 28 June 2017; posted 21 July 2017 (Doc. ID 292922); published 21 August 2017

We theoretically propose blue-detuned optical trapping for neutral atoms via strong near-field interfacing in a plasmonic nanohole array. The optical field at resonance forms a nanoscale-trap potential with an FWHM of 200 nm and about ~ 370 nm away from the nanohole; thus, a stable 3D atom trapping independent of the surface potential is demonstrated. The effective trap depth is more than 1 mK when the optical power of trapping light is only about 0.5 mW, while the atom scattering rate is merely about 3.31 s^{-1} , and the trap lifetime is about 800 s. This compact plasmonic structure provides high uniformity of trap depths and a two-layer array of atom nano-traps, which should have important applications in the manipulation of cold atoms and collective resonance fluorescence. © 2017 Chinese Laser Press

OCIS codes: (240.6680) Surface plasmons; (230.4555) Coupled resonators; (020.1335) Atom optics; (020.7010) Laser trapping.

<https://doi.org/10.1364/PRJ.5.000436>

1. INTRODUCTION

Trapping and cooling neutral atoms, which is an active field in atomic optics, is important to achieve the Bose–Einstein condensate (BEC), test basic physical laws, and measure basic physical constants in a more accurate manner [1–5]. In recent years, optical dipole traps have become a widely used tool for trapping neutral atoms [5]. The dipole trap mainly uses the gradient light intensity formed by the focused light field to produce a dipole effect on a neutral atom. In the more used red-detuned traps, the atoms are trapped in the position with the strongest light intensity under attractive potential [6,7]. However, even in the case of a far-off resonance optical dipole trap (FORT) light, the atom will be subjected to large photon's Rayleigh and Raman scattering, resulting in obvious destruction of atomic coherence and heating effect [5]. Simultaneously, the atomic energy level usually has a serious optical frequency shift in the strongest light intensity position [8]. In contrast, for the blue-detuned traps [9–11], the atoms are trapped in the weakest position under the exclusion potential; thus, the impact of the blue-detuned light is very small. But compared with the red-detuned traps, the construction of the blue-detuned traps is often more complex [4,6–11]. Later on, the researchers proposed the use of an evanescent wave method to achieve atom trapping [12–17]. Furthermore, in order to create a stable trapping potential, two-color traps (a red-detuned and a blue-detuned light) with

a relatively large power and appropriate power ratio are needed because of the attractive van der Waals forces in the structure surface, which undoubtedly increases the difficulty of the experiments [12–17]. Therefore, to trap atoms stably in a compact structure with very low power, blue-detuned light is needed.

As we know, surface plasmon polaritons (SPPs) are optical resonance originating from excitation of free electron oscillations at the surface of metals [18]. SPPs are in a subwavelength scale with great local field enhancement effect, and they can break through a diffraction limit, which has many important applications in the fields of materials, energy, biology, and information [19–24]. Thus, combining the neutral atom trapping with nanoplasmonic structures would open the possibility of achieving ultracompact functional optical components in highly integrated optics. For example, Murphy *et al.* proposed a suspended Ag sphere dimer and a parabolic plasmonic structure for isolated atom trapping [25,26], respectively. Gullans *et al.* studied a kind of nanoplasmonic lattices for atom arrays trapping [27], which is of great significance in studying atom–atom interactions, resonance fluorescence, and multi-site-selective [28–31]. However, the structures proposed in the above works must overcome the influence of van der Waals potentials in order to obtain stable trapping; further, the structures are difficult for manufacture and integration [25–28].

In this paper, we propose a compact plasmonic structure for rubidium atom (^{87}Rb) trapping using a periodic nanohole array in a homogeneous metallic film. Simulation results show that two traps with minimum potentials are formed, which are ~ 370 nm away from the nanohole due to the hotspots arising. A blue-detuned circular polarized light, which also makes the system resonant, ensures 3D traps for ^{87}Rb atoms. Only about 0.5 mW of incident optical power with a trap depth about 1 mK can be achieved with atom scattering rates 3.31 s^{-1} and a trap lifetime 800 s. A stable two-layer 3D atom trapping independent on the surface potential is demonstrated, while only one layer trapping dependent on surface potential heavily was previously obtained [28–31]. This kind of plasmonic structure is easy to fabricate and integrate into a hybrid system; moreover, this type of atom trapping method, based on surface plasmon, provides a promising possibility for atomic on-chip integration.

2. STRUCTURE AND SIMULATION RESULTS

Periodic arrays of subwavelength holes in metallic films exhibit an extraordinary optical transmission effect, which will generate large local field enhancement near the nanoholes [23]. Here, we consider this effect of such fields on atomic motion. A plasmon resonant field that is blue-detuned from the atomic resonance can produce a remarkable repulsive force of atoms, and a trap minimum about hundreds of nanometers from the structure surface will come into being [26,27]. To illustrate our approach, we consider a scheme of an array of nanoholes (air) in metallic (Au) films, as shown in Fig. 1(a). The inset shows the unit cell of the presented nanohole arrays and the geometrical

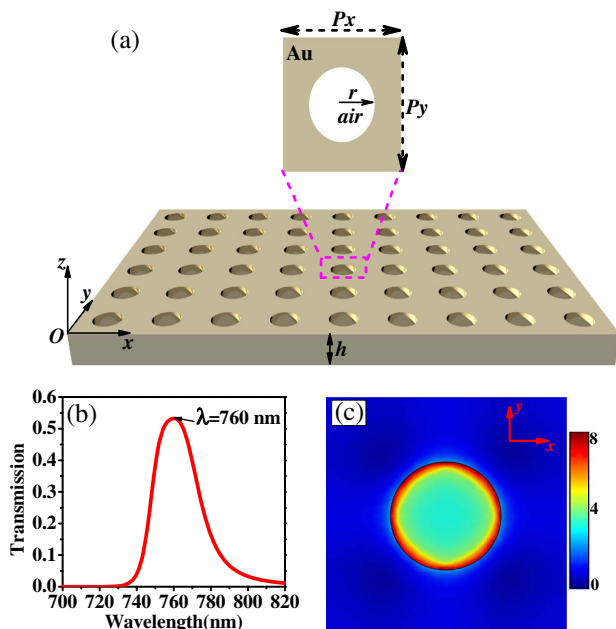


Fig. 1. (a) Schematic of the array of nanoholes in a metallic film. Inset shows the unit cell of the presented nanohole arrays and the geometrical parameter symbols. (b) Simulation results of the normalized zero-order transmission spectrum. (c) Field distribution of $|E|$ in the nanohole at the air–gold interface when a 760 nm laser illuminates from the $-z$ direction.

parameter symbols. The structure is periodic in the x – y plane, while only a single unit layer is considered in the z direction. The main parameters of the unit cell are as follows: $P_x = P_y = 700$ nm, $r = 160$ nm, and $h = 400$ nm, respectively. The numerical calculations are carried out using COMSOL Multiphysics based on the finite element method. The transmission, T , is calculated by integrating the Poynting vector over the upper surface and normalizing to that obtained in the absence of the metal film [32]. The permittivity of Au as a function of the wavelength (λ) is taken from the literature [33] and expanded using the method of interpolation. A circular polarization light is normal incident from the $-z$ direction at infinity, and the calculated normalized zero-order transmission spectrum is displayed in Fig. 1(b). It is obviously observed that a resonant peak with $\lambda = 760$ nm emerges in the transmission spectrum. The transmission efficiency, about 55%, is attributed to the extraordinary optical transmission effect [23]. As a laser beam of $\lambda = 760$ nm illuminates from the $-z$ direction, the hot spots [34] emerge around the edge of the nanohole, as depicted by the field distributions of $|E|$ in Fig. 1(c). A periodic arrangement of air holes has Bragg scattering to the SPPs, which imposes a reciprocal lattice vector of the periodicity to the phase-matching condition [35]. Thus, the incident wave can satisfy the phase-matching condition and excite the SPPs, which concentrates at the edge of the hole resulting in the hot spots. This way of exciting SPPs (based on periodic nanoholes) is much easier than using the Kretschmann structure [17] and does not depend on the thickness of the metal.

In order to study the spatial electric field distributions of the system, the field distributions of $|E|$ in the x – z plane at $y = 0$ nm at the resonant wavelength $\lambda = 760$ nm is shown in Fig. 2(a). It is observed that two minimums of electric fields emerge (trap center), as indicated by the two green arrows in Fig. 2(a). The appearance of these two minimums can be attributed to the hot spots arising, which results from the near-field

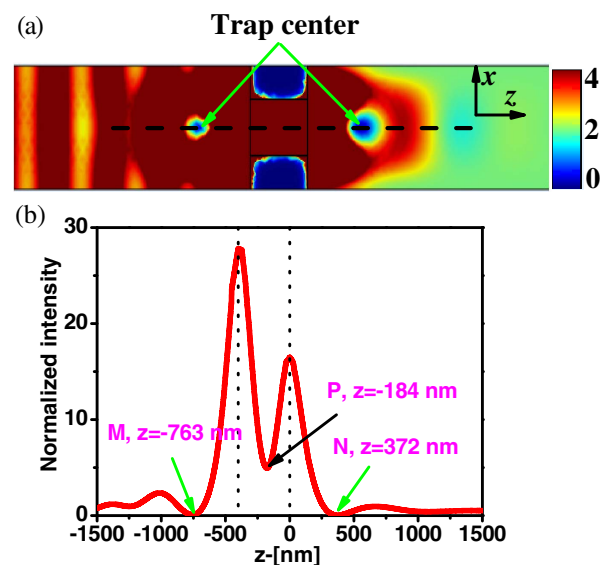


Fig. 2. (a) Field distributions of $|E|$ in the x – z plane when y is 0 nm. (b) Normalized intensity distributions of $|E|^2$ along the dark dashed line in (a).

scattering of light by an array of plasmonic nanoholes [27]. For a more detailed description of the system field distribution, the normalized intensity ($|E|^2$) along the dark dashed line in Fig. 2(a) is given in Fig. 2(b). Herein, the electric field E is the superposition of the evanescent field (SPPs) and the spatial electric field through the nanoholes. The simulation results above indicate that the spatial electric field distribution can form two intensity minima, which implies the blue-detuned optical trap for neutral atom manipulation. Here, the resonant wavelength $\lambda = 760$ nm is chosen to be blue-detuned to the D_2 line of rubidium, which repels the atoms from the high light intensity due to the optical dipole force to the minimum. In addition, the two trap centers are both about 370 nm away from the surface, which greatly reduces the effects of van der Waals forces [13–16,25–27,36].

3. TRAPPING POTENTIALS

A neutral atom can be trapped in electric field intensity minima via optical dipole forces with blue-detuned light [5]. The total trapping potential U_{tot} for an atom is the sum of the repulsive optical dipole potential U_{opt} and the attractive Casimir–Polder potential U_{CP} :

$$U_{\text{tot}} = U_{\text{opt}} + U_{\text{CP}}, \quad (1)$$

where the optical dipole potential U_{opt} that a neutral atom with atomic state i and Zeeman level m_i experiences in an electric field \mathbf{E} is given by [5,7,36]

$$U_{\text{opt}} = -\frac{1}{4}\alpha|E|^2. \quad (2)$$

Here, α is a reduced polarizability, which can be described by [7]

$$\alpha = 6\pi\epsilon_0 c^3 \sum_{k,m_i} \frac{A_{ki}(2J_k + 1)}{\omega_{ik}^2(\omega_{ik}^2 - \omega^2)} \begin{pmatrix} J_i & 1 & J_k \\ m_i & P & -m \end{pmatrix}. \quad (3)$$

Here ϵ_0 is the permeability of vacuum and c is the speed of light. The expression within the large parentheses denotes a Wigner 3-j symbol. A_{ki} are the Einstein coefficients, $\omega_{ik}/(2\pi)$ is the transition frequencies and J is the involved angular momenta. In our case, $\alpha \approx -7.87 \times 10^{-38} \text{ F} \cdot \text{m}^2$. Therefore, the dipole potentials can be obtained according to the electric field intensity distributions in the previous section. U_{CP} is surface effect, which can play an important role in the trap characteristics, when the atom is close to the structure surface. According to the description in Ref. [37], we know that Casimir–Polder forces and van der Waals forces have the similar surface effects on trapped atoms within a distance about $d < 100$ nm and decrease fast away from the surface [38]. Here, we choose the Casimir–Polder potential as the surface effects, which is given by

$$U_{\text{CP}} = -K_4 \cdot [d^3(d+l)]^{-1}, \quad (4)$$

with the length scale $l = 780/(2\pi)$ nm corresponding to the D_2 line of ^{87}Rb atoms. d is the distance from the Au surface to the atom. The value of the Casimir–Polder coefficient K_4 is $5 \times 10^{-55} \text{ J} \cdot \text{m}^4$ [39].

According to above equations and Fig. 2(b), we calculated the total potential along the dark dashed line in Fig. 2(a), as

displayed in Fig. 3(a). Throughout this paper, the incident blue detuned laser power is set as $P_0 = 1$ mW. Herein, the $U_{\text{CP}} \approx -0.001$ mK and can be neglected in calculating the U_{tot} due to the structure being hollow. Therefore, the total potential has similar distributions as the electric field intensity distributions, when compared with Figs. 2(b) and 3(a). We define that the effective trap depth U_{eff} of the dipole trap is the potential difference between the potential minimum that the trapped atoms can escape and the U_{tot} . From Fig. 3(a), we know that the possible trapping positions are the regions in the x - y plane of $z = -763$ nm (point M, $U_{\text{tot}} = 0.21$ mK, $U_{\text{eff}} = 5.00$ mK), $z = -184$ nm (point P, $U_{\text{tot}} = 11.50$ mK, $U_{\text{eff}} = 25.30$ mK) and $z = 372$ nm (point N, $U_{\text{tot}} = 0.10$ mK, $U_{\text{eff}} = 2.02$ mK) lie. In order to understand the 3D trapping possibility of the system, these three regions are investigated in the following.

First, we begin with the point P ($z = -184$ nm). The total potential U_{tot} in the x - y plane will be greatly affected by the U_{CP} because point P is inside the nanohole (range from $-b$ to 0). According to Eqs. (1), (2), and (4), we calculate the potential distributions in the x - y plane at $z = -184$ nm, which is displayed in Fig. 3(b). Here, U_x and $U_{\text{tot}-x}$ represent the optical dipole potential and the total potential along the x direction, respectively. It is obviously seen that a potential peak, point P , emerges in the x - y plane. That is to say, the ^{87}Rb atoms that reach point P from the z direction will diffuse around along the x direction and will eventually be adsorbed on the metal wall. Namely, no stable trapping potential exists.

Then we investigate the trapping property for point N in the x - y plane ($z = 372$ nm), the contour plot of the total potential distributions of ^{87}Rb for a unit cell is displayed in Fig. 4(a). It is clearly seen that this periodic nanohole array structure provides a positive finite potential. The minimum potential of the trapping center is only about $U_{\text{tot}} = 0.10$ mK ($z = 372$ nm), and there is a point with a maximum potential that the trapped atom can escape about 2.87 mK for the x or y direction, which can contribute to the effective trap depth about $U_{\text{eff}} = 2.77$ mK. Taking the trapping potential for the z direction into consideration, the effective dipole trap depth is $U_{\text{eff}} = 2.02$ mK. That is to say, about 0.5 mW of incident power can generate 1 mK trap depth, which is

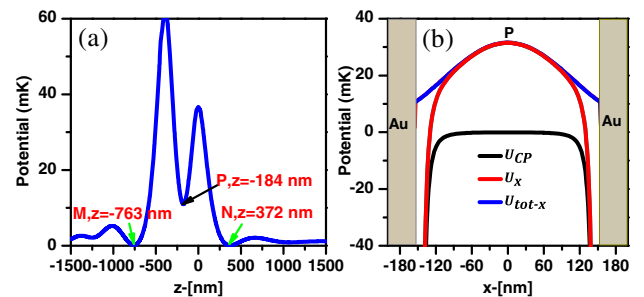


Fig. 3. (a) Calculated total potential along the dark dashed line in Fig. 2(a). (b) Potential distributions for point P in the x - y plane. U_x and $U_{\text{tot}-x}$ represent the optical dipole potential and the total potential along the x direction, respectively. The incident optical power $P_0 = 1$ mW.

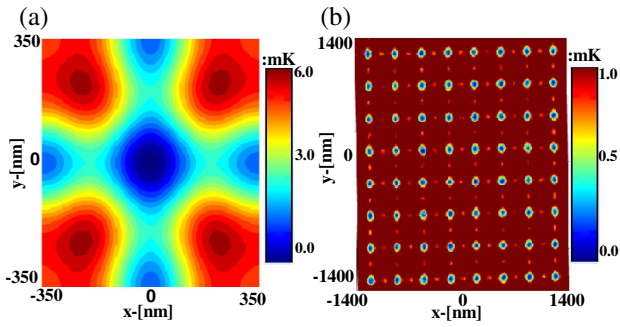


Fig. 4. (a) Contour plot of a trapping total potential in the x - y plane at $z = 372$ nm for a unit cell. (b) Periodic arrays.

commonly used in single-atom trapping experiments [5]. Using the near-field scattering effect of the periodic nanoholes, we can achieve 3D trapping for a single atom in each trap center, which is more stable than 2D trapping [11]. For a same $U_{\text{eff}} = 1$ mK, this optical power is much smaller than in previous reports with 6 mW in Ref. [7], 80 mW in Ref. [8]. Ultra-low power can reduce the heating effect on the atom and increase the trapping lifetime. In addition, the FWHM of the nanotrap is about 200 nm, which is small enough to trap a single atom [7]. To the best of our knowledge, atom trapping based on blue-detuned light without surface potentials effects has scarcely been previously reported. For point M ($z = -763$ nm), there are similar potential distributions except for the specific trapping depth value (the minimum potential of the trapping center is about $U_{\text{tot}} = 0.21$ mK and about $U_{\text{eff}} = 5.17$ mK for the x or y direction and $U_{\text{eff}} = 5.00$ mK for the z direction).

4. ATOM TRAPPING VIABILITY

To quantify the viability of an atom trap, the scattering rates should be determined. Atoms will be heated by the laser field and will undergo a momentum recoil due to photo scattering, which can result in atom loss from the atom trap. For an atom in a dipole trap, the scattering rates, Γ_{sc} , is given as [5,36]

$$\Gamma_{\text{sc}} = \frac{\Gamma U_{\text{tot}}}{\Delta \hbar}. \quad (5)$$

Here, Γ is the dipole transition matrix element between the ground $|g\rangle$ and $|e\rangle$ excited state, \hbar is the reduced Planck's constant, and Δ is the detuning. For ^{87}Rb , we can assume that the major contributions to Γ_{sc} are from the dipole transition rates from $S_{1/2}$ to the $P_{1/2}$ and $P_{3/2}$ excited states [36]. With these simplifications Eq. (5) becomes

$$\Gamma_{\text{sc}} = \left(\frac{\Gamma_{1/2}}{3\Delta_{1/2}} + \frac{2\Gamma_{3/2}}{3\Delta_{3/2}} \right) \frac{U_{\text{tot}}}{\hbar}, \quad (6)$$

where $\Gamma_{1/2}$ and $\Gamma_{3/2}$ are the dipole transition matrix elements from the $S_{1/2}$ to the $P_{1/2}$ and $P_{3/2}$ excited states, respectively. For an effective trap depth 1 mK, the calculated scattering rate is only about 3.31 s^{-1} , which is a much lower value compared with previous reports, about 98.78 s^{-1} in Ref. [36] and 6100 s^{-1} in Ref. [40]. Each scattered photon from either field contributes

some recoil energy to the atom. This will lead to a loss of atoms from the dipole trap. A trap lifetime is given as [36,40]

$$\tau_c = \frac{U_{\text{eff}}}{2E^r\Gamma_{\text{sc}}}, \quad (7)$$

where $E^r = \hbar^2/(8m\pi^2\lambda^2)$ is the recoil energy associated with a blue photon, and m is the atomic mass of ^{87}Rb . A trap lifetime about 800 s is obtained with $U_{\text{eff}} = 1$ mK, which is about 2000 times compared with Ref. [40] in a same trap depth.

At last, we show total potential distributions in the x - y plane at $z = 372$ nm of the periodic arrays in Fig. 4(b). It is obviously observed that the periodic structure guarantees the uniformity of trap depths in each unit cell, which greatly reduces the detection error due to the variance of cooling efficiency and the photon scattering rate from each atom. Compared with the multi-beam trapping [9,10], only a bunch of ultra-low-power (0.5 mW) blue-detuned light is required in our proposal, which is more compact and easier to be controlled. The distance between trap wells is the same as the period of the system, and the trap depth of each well can be adjusted by adding nonlinear materials in the nanoholes [41]. Surely, at $z = -763$ nm, the atom array also can be trapped. This kind of two-layer array of atom trapping is on both sides of the structure, which has not been previously reported, to the best of our knowledge. Such plasmonic structure is easy to fabricate and integrate into a hybrid system [42,43]. This two-layer array of such atom nanotraps could have applications for site-selective manipulation, resonance fluorescence of cold atoms, and multi-bit operation within a small volume.

5. CONCLUSION

In conclusion, we have proposed a compact plasmonic structure for neutral rubidium atoms trapping with a blue-detuned light, which produces an array of potential minima in the near field. The resonant wavelength of the system is used as the trapping light for neutral atoms, which can greatly reduce the optical power due to the SPPs excited. The FWHM of the nanotrap is about 200 nm, and the trap center is about 370 nm away from the nanohole surface, which effectively avoids the effects of van der Waals forces, and a stable 3D atom trapping independent on the surface potential is demonstrated. The effective trap depth is more than 1 mK when the optical power of the trapping light is only about 0.5 mW. The calculated scattering rate is merely about 3.31 s^{-1} , and a trap lifetime is about 800 s. Moreover, the periodic system provides high uniformity of trap depths, which greatly diminishes the detection error due to the variance of cooling efficiency and the photon scattering rate from each atom. This kind of plasmonic structure is easy to fabricate and integrate into a hybrid system, and such two layers of atom nanotraps are of importance for complex functional devices, resonance fluorescence, and multiple access selection in highly integrated photonic circuits and quantum information processing.

Funding. National Key Basic Research Program (2013CB328700); National Natural Science Foundation of China (NSFC) (11525414, 11374025, 91221304).

Acknowledgment. The authors would like to thank Prof. Xiaoyong Hu, and Mr. You Wu from Peking University for their fruitful discussions.

REFERENCES

1. E. Arimondo, W. D. Phillips, and F. Strumia, *Laser Manipulation of Atoms and Ions* (North Holland, 1991).
2. W. D. Phillips, "Laser cooling and trapping of neutral atoms," *Rev. Mod. Phys.* **70**, 721–741 (1998).
3. J. Fortagh and C. Zimmermann, "Magnetic microtraps for ultracold atoms," *Rev. Mod. Phys.* **79**, 235–289 (2007).
4. J. P. Yin, "Realization and research of optically-trapped quantum degenerate gases," *Phys. Rep.* **430**, 1–116 (2006).
5. R. Grimm, M. Weidemüller, and Y. B. Ovchinnikov, "Optical dipole traps for neutral atoms," *Adv. At. Mol. Opt. Phys.* **42**, 1–39 (2000).
6. S. Kato, S. Chonan, and T. Aoki, "High-numerical-aperture micro-lensed tip on an air-clad optical fiber," *Opt. Lett.* **39**, 773–775 (2014).
7. P. F. Zhang, G. Li, and T. C. Zhang, "Subwavelength optical dipole trap for neutral atoms using a microcapillary tube tip," *J. Phys. B* **50**, 045005 (2017).
8. P. Xu, X. He, J. Wang, and M. Zhan, "Trapping a single atom in a blue detuned optical bottle beam trap," *Opt. Lett.* **35**, 2164–2166 (2010).
9. M. J. Piotrowicz, M. Lichtman, K. Maller, G. Li, S. Zhang, L. Isenhower, and M. Saffman, "Two-dimensional lattice of blue-detuned atom traps using a projected Gaussian beam array," *Phys. Rev. A* **88**, 013420 (2013).
10. P. Zemanek and C. J. Foot, "Atomic dipole trap formed by blue detuned strong Gaussian standing wave," *Opt. Commun.* **146**, 119–123 (1998).
11. N. T. Phuong Lan, D. T. Thuy Nga, and N. A. Viet, "Trapping cold atoms using surface plasmons with phase singularities generated by evanescent Bessel beams," *J. Phys. Conf. Ser.* **627**, 012017 (2015).
12. M. Hammes, D. Rychtarik, B. Engeser, H. C. Nagerl, and R. Grimm, "Evanescent-wave trapping and evaporative cooling of an atomic gas at the crossover to two dimensions," *Phys. Rev. Lett.* **90**, 173001 (2003).
13. T. Nieddu, V. Gokhroo, and S. N. Chormaic, "Optical nanofibers and neutral atoms," *J. Opt.* **18**, 053001 (2016).
14. E. Vetsch, D. Reitz, G. Sague, R. Schmidt, S. T. Dawkins, and A. Rauschenbeutel, "Optical interface created by laser-cooled atoms trapped in the evanescent field surrounding an optical nanofiber," *Phys. Rev. Lett.* **104**, 203603 (2010).
15. A. Goban, K. S. Choi, D. J. Alton, D. Ding, C. Lacroute, M. Pototschnig, and T. Thiele, "Demonstration of a state-insensitive, compensated nanofiber trap," *Phys. Rev. Lett.* **109**, 033603 (2012).
16. N. V. Corzo, B. Gouraud, A. Chandra, A. Goban, A. S. Sheremet, D. V. Kupriyanov, and J. Laurat, "Large Bragg reflection from one-dimensional chains of trapped atoms near a nanoscale waveguide," *Phys. Rev. Lett.* **117**, 133603 (2016).
17. C. R. Bennett, J. B. Kirk, and M. Babiker, "Theory of evanescent mode atomic mirrors with a metallic layer," *Phys. Rev. A* **63**, 033405 (2001).
18. W. L. Barnes, A. Dereux, and T. W. Ebbesen, "Surface plasmon sub-wavelength optics," *Nature* **424**, 824–830 (2003).
19. Y. J. Xiong, J. Y. Chen, B. Wiley, Y. N. Xia, Y. D. Yin, and Z. Y. Li, "Size-dependence of surface plasmon resonance and oxidation for Pd nanocubes synthesized via a seed etching process," *Nano Lett.* **5**, 1237–1242 (2005).
20. S. Link and M. A. El-Sayed, "Spectral properties and relaxation dynamics of surface plasmon electronic oscillations in gold and silver nanodots and nanorods," *J. Phys. Chem. B* **103**, 8410–8426 (1999).
21. Z. W. Liu, J. M. Steele, W. Sritravanich, Y. Pikus, C. Sun, and X. Zhang, "Focusing surface plasmons with a plasmonic lens," *Nano Lett.* **5**, 1726–1729 (2005).
22. H. Dittbacher, A. Hohenau, D. Wagner, U. Kreibig, M. Rogers, F. Hofer, F. R. Aussenegg, and J. R. Krenn, "Silver nanowires as surface plasmon resonators," *Phys. Rev. Lett.* **95**, 257403 (2005).
23. T. W. Ebbesen, H. J. Lezec, H. Ghaemi, T. Thio, and P. A. Wolf, "Extraordinary optical transmission through sub-wavelength hole arrays," *Nature* **391**, 667–669 (1998).
24. K. A. Willets and R. P. Van Duyne, "Localized surface plasmon resonance spectroscopy and sensing," *Annu. Rev. Phys. Chem.* **58**, 267–297 (2007).
25. D. E. Chang, J. D. Thompson, H. Park, V. Vuletic, A. S. Zibrov, P. Zoller, and M. D. Lukin, "Trapping and manipulation of isolated atoms using nanoscale plasmonic structures," *Phys. Rev. Lett.* **103**, 123004 (2009).
26. B. Murphy and L. V. Hau, "Electro-optical nanotraps for neutral atoms," *Phys. Rev. Lett.* **102**, 033003 (2009).
27. M. Gullans, T. Tiecke, D. E. Chang, J. Feist, J. Thompson, J. Cirac, P. Oller, and M. D. Lukin, "Nanoplasmonic lattices for ultracold atoms," *Phys. Rev. Lett.* **109**, 235309 (2012).
28. A. Gonzalez, C. Hung, D. E. Chang, J. Cirac, and H. Kimble, "Subwavelength vacuum lattices and atom-atom interactions in two-dimensional photonic crystals," *Nat. Photonics* **9**, 320–325 (2015).
29. H. Tamura, T. Unakami, J. He, Y. Miyamoto, and K. Nakagawa, "Highly uniform holographic microtrap arrays for single atom trapping using a feedback optimization of in-trap fluorescence measurements," *Opt. Express* **24**, 8132–8141 (2016).
30. T. N. Bandi, V. G. Minogin, and S. N. Chormaic, "Atom microtraps based on near-field Fresnel diffraction," *Phys. Rev. A* **78**, 013410 (2008).
31. C. Garcia-Segundo, H. Yan, and M. S. Zhan, "Atom trap with surface plasmon and evanescent field," *Phys. Rev. A* **75**, 030902 (2007).
32. L. Lin, L. B. Hande, and A. Roberts, "Resonant nanometric cross-shaped apertures: single apertures versus periodic arrays," *Appl. Phys. Lett.* **95**, 201116 (2009).
33. P. B. Johnson and R.-W. Christy, "Optical constants of the noble metals," *Phys. Rev. B* **6**, 4370–4379 (1972).
34. F. Zhao, J. Zeng, M. Arnob, P. Sun, J. Q. P. Motwani, M. Gheewala, C. Li, A. Paterson, U. Strych, B. Raja, R. Willson, J. Wolfe, T. Lee, and W. Shih, "Monolithic NPG nanoparticles with large surface area, tunable plasmonics, and high-density internal hot-spots," *Nanoscale* **6**, 8199–8207 (2014).
35. M. Luo and Q. Liu, "Extraordinary transmission of a thick film with a periodic structure consisting of strongly dispersive materials," *J. Opt. Soc. Am. B* **28**, 629–636 (2011).
36. M. Daly, V. G. Truong, C. F. Phelan, K. Deasy, and S. N. Chormaic, "Nanostructured optical nanofibers for atom trapping," *New J. Phys.* **16**, 053052 (2014).
37. C. Lacroute, K. Choi, A. Goban, D. Alton, D. Ding, N. Stern, and H. J. Kimble, "A state-insensitive, compensated nanofiber trap," *New J. Phys.* **14**, 023056 (2012).
38. D. E. Chang, K. Sinha, J. M. Taylor, and H. J. Kimble, "Trapping atoms using nanoscale quantum vacuum forces," *Nat. Commun.* **5**, 4343 (2014).
39. C. Stehle, H. Bender, C. Zimmermann, D. Kern, M. Fleischer, and S. Slama, "Plasmonically tailored micropotentials for ultracold atoms," *Nat. Photonics* **5**, 494–498 (2011).
40. J. P. Burke, S. Chu, G. Bryant, C. J. Williams, and P. S. Julienne, "Designing neutral-atom nanotraps with integrated optical waveguide," *Phys. Rev. A* **65**, 043411 (2002).
41. Z. Chai, X. Hu, H. Yang, and Q. Gong, "Chip-integrated all-optical diode based on nonlinear plasmonic nanocavities covered with multicomponent nanocomposite," *Nanophotonics* **6**, 329–339 (2017).
42. F. Y. Gan, Y. Wang, C. Sun, G. Zhang, H. Li, J. Chen, and Q. Gong, "Widely tuning surface plasmon polaritons with laser-induced bubbles," *Adv. Opt. Mater.* **5**, 1600545 (2017).
43. H. Gao, J. Henzie, and T. Odom, "Direct evidence for surface plasmon-mediated enhanced light transmission through metallic nanohole arrays," *Nano Lett.* **6**, 2104–2108 (2006).